Hindawi
Advances in Meteorology
Volume 2020, Article ID 6726347, 11 pages
https://doi.org/10.1155/2020/6726347

Research Article

Impact of the Westerly Jet on Rainfall/Runoff in the Source Region of the Yangtze River during the Flood Season

Xin Lai,[1,2] **Yuanfa Gong**,[1] **Sixian Cen**,[3] **Hui Tian**,[2] **and Heng Zhang**[4]

[1]*School of Atmospheric Sciences, Plateau Atmosphere and Environment Key Laboratory of Sichuan Province, Joint Laboratory of Climate and Environment Change, Chengdu University of Information Technology, Chengdu 610225, China*
[2]*Key Laboratory for Land Surface Process and Climate Change in Cold and Arid Regions, Chinese Academy of Sciences, Lanzhou 730000, China*
[3]*Chengdu Institute of Plateau Meteorology, China Meteorology Administration, Heavy Rain and Drought-Flood Disasters in Plateau and Basin Key Laboratory of Sichuan Province, Chengdu 610072, China*
[4]*Bazhong Meteorological Office of Sichuan Province, Bazhong 636000, China*

Correspondence should be addressed to Xin Lai; nacylai@cuit.edu.cn

Received 19 August 2019; Revised 11 January 2020; Accepted 4 February 2020; Published 21 March 2020

Academic Editor: Herminia García Mozo

Based on runoff data collected at the Zhimenda station, reanalysis data from the National Centers of Environmental Prediction/National Centers of Atmospheric Research (NCEP/NCAR), and observation data from ground stations in China, this study analyzes the characteristics of changes in runoff in the source region of the Yangtze River (SRYR) during the flood season (from July to September), the relationship between runoff and antecedent rainfall, and the impact of the westerly jet (WJ) on rainfall in the coastal zone of the SRYR. The results show the following. The runoff in the SRYR displays a significant interannual and interdecadal variability. The runoff in the SRYR during the flood season is most closely related to 15-day (June 16 to September 15) antecedent rainfall in the coastal zone of the SRYR. In turn, the antecedent rainfall in the coastal zone of the SRYR is mainly affected by the intensity of the simultaneous WJ over a key region (55–85°E, 45–55°N). When the intensity of the WJ over the key region is greater (less) than normal, the jet position moves northward (southward), and the easterly (westerly) wind anomalies over the region to the west of the SRYR become unfavorable (favorable) to the transport of water vapor from high-latitude regions to the SRYR. In addition, the southerly wind over the equatorial region cannot (can) easily advance northward, which is unfavorable (favorable) to the northward transport of water vapor from the low-latitude ocean. Hence, these conditions result in a decrease (increase) in the water vapor content in the SRYR. Furthermore, the convergence (divergence) anomalies in the upper level and the divergence (convergence) anomalies in the lower level result in the descending (ascending) motion over the SRYR. These factors decrease (increase) the rainfall, thereby decreasing (increasing) the runoff in the SRYR during the flood season.

1. Introduction

The Yangtze River originates at the terminuses of the glaciers on Geladaindong Mountain in the middle section of the Tanggula Mountain Range in Qinghai Province. The headwaters consist mainly of three rivers, namely, the Dangqu River (southern source), the Tuotuo River (main source), and the Chumar River (northern source). The Tuotuo River converges with the Dangqu River to form the Tongtian River, which flows southeastward and converges with the Batang River near Yushu County in Qinghai Province to form the Jinsha River. Hydrologically, the region upstream of the Zhimenda hydrological station is generally treated as the source region of the Yangtze River (SRYR). Changes in runoff in the SRYR not only affect the regional ecological environment but also significantly affect the water resources in the middle and lower reaches of the Yangtze River. Therefore, a number of researchers have studied the characteristics of runoff in the SRYR [1–5]. The runoff in the SRYR is mainly concentrated between May and September. From the 1960s to the 1990s, the runoff in the SRYR exhibited an overall decreasing trend with four main stages,

namely, a wet stage, followed by a dry stage, another wet stage, and another dry stage. The 1990s was a relatively particularly dry stage [6–8]. The SRYR entered a wet stage in approximately 2005 [9]. However, these studies only examined relatively short periods of time. By reconstructing the runoff of the Tongtian River since 1485, Qin et al. [10] analyzed the long-term characteristics of its changes. Many factors could influence runoff in the SRYR. For example, a precipitation increase could cause the runoff in the SRYR to increase, whereas an evaporation increase could cause the runoff in the SRYR to decrease. The heating of the Tibetan Plateau (TP), enhanced plateau monsoon, and enhanced glacier melting could also increase the runoff in the SRYR [2, 5, 11–13]. However, precipitation is the principal factor that affects the runoff [14, 15]. The relationship between precipitation and periodic fluctuations in runoff in the SRYR is much more significant than that between the temperature and runoff; in addition, the annual runoff also corresponds to annual precipitation in terms of interdecadal changes and years when abrupt changes take place [16, 17]. Thus, precipitation is the principal factor that affects the runoff in the SRYR.

The upper-level westerly jet (WJ) is a planetary-scale atmospheric circulation system in the upper troposphere and is an important circulation system that affects the weather and climate in East Asia [18–23]. Hence, numerous researchers have studied the WJ [24–30]. Changes in the position and intensity of the WJ significantly affect the weather and climate in China. With regard to the influence of changes in the position of the WJ, most research has emphasized the influence of meridional movement. On the one hand, the meridional movement of the WJ can influence the Meiyu occurrence. For example, Tao et al. [31] found that the start and end of East Asian Meiyu are related to two northward jumps of the southern branch of the WJ over Asia between June and July. The second northward jump of the southern branch of the WJ occurs before Meiyu in the Jianghuai region of China [32]. On the other hand, the southward and northward jumps of the subtropical WJ in summer also affect the location of the rainband. In June, precipitation anomalies mainly occur over the sea surface south of Japan. In July, when the WJ jumps northward, the rainband moves northward from the middle and lower reaches of the Yangtze River to the Huai River and the region north of it [33, 34]. Additionally, the meridional movement of the subtropical WJ can significantly influence summer precipitation in China. In summer, the subtropical WJ moves southward, resulting in increased precipitation in the Yangtze-Huai River basin and the Jiangnan region [18, 20, 23, 26, 35] and decreased precipitation in Northeast China [36, 37]. The zonal movement of the subtropical WJ can also influence Meiyu. Zhang et al. noted that the eastward and westward movements of the subtropical WJ affect the start and end of the Meiyu period [38]. In addition, changes in the shape of the subtropical WJ in the eastern and western directions also affect the spatial distribution of precipitation in the middle and lower reaches of the Yangtze River during the Meiyu period [39]. If the center of the East Asian subtropical WJ is located relatively westward in January and its axis is situated relatively southward between April and May, the year may be a rich Meiyu year [40]. Furthermore, many researchers have studied the influence of changes in the strength of the subtropical WJ. Liang and Liu [41] found that when the southern branch of the WJ in winter is relatively strong (weak), there will be relatively greater precipitation in South China in the following spring and in North China in the following summer. Li and Zhang pointed out that a strong subtropical WJ can increase the precipitation in the Meiyu period [42]. Wang and Zuo further pointed out that a strong subtropical WJ decreases the precipitation in the Yangtze River basin in midsummer (16 July–14 August) [19]. Evidently, the subtropical WJ has a significant impact on precipitation in China, especially East China. The SRYR is located in the region impacted by the westerlies, but relatively few studies have been conducted to examine the influence of the WJ on the precipitation in the SRYR. In view of this, this study aims to investigate the impact of the WJ on rainfall in the SRYR and analyze its impact on runoff in the SRYR, with the goal of providing a certain basis for protection of the ecological environment of the SRYR.

This paper is organized as follows. Brief descriptions of the data and method are provided in Section 2. Characteristics of changes in runoff in the SRYR are analyzed in Section 3. Correlation analyses of runoff and rainfall in the SRYR during the flood season are provided in Section 4. The impact of the WJ on rainfall in the SRYR is analyzed in Section 5. The impact of the intensity of the WJ over the key region on atmospheric circulation patterns is investigated in Section 6. The impact of the intensity of the WJ over the key region on water vapor transport is investigated in Section 7. Section 8 discusses the major conclusions of this study.

2. Data and Methods

2.1. Data. The hydrological data used in this study were monthly runoff observation data collected from 1956 to 2012 at the Zhimenda station. In addition, the runoff at the Zhimenda station (Figure 1) was treated as the runoff in the SRYR. The rainfall data used in this study were complete daily observation data collected at 109 stations (Figure 1) in China between 85°E and 105°E and between 25°N and 40°N from 1961 to 2012 and were provided by the National Meteorological Information Center of the China Meteorological Administration. The daily reanalysis data, including surface pressure, zonal wind (u), meridional wind (v), vertical velocity (w), and specific humidity (q), are derived from the National Centers of Environmental Prediction/National Centers of Atmospheric Research (NCEP/NCAR) reanalysis data, with a horizontal resolution of 2.5°. Fang et al. [43, 44] noted that the NCEP/NCAR data for East Asia for the period 1958–1967 have substantial quality issues. Therefore, the period 1971–2012 was selected for analysis in this study.

2.2. Methods. The vertically integrated water vapor flux vector can be expressed as

$$Q = Q_\lambda \vec{i} + Q_\phi \vec{j}. \quad (1)$$

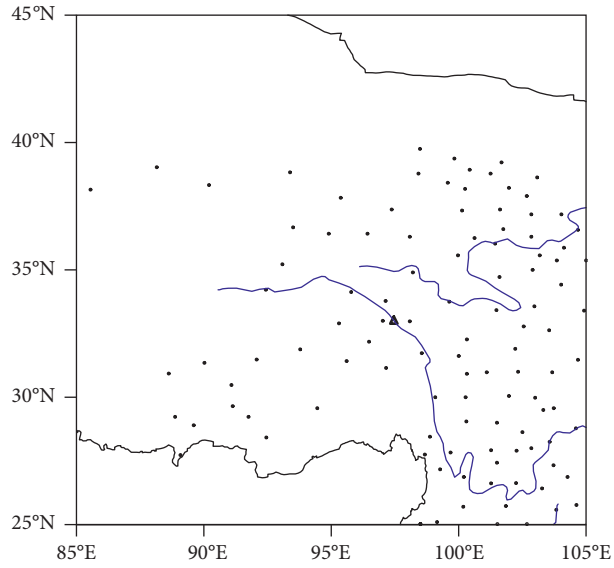

Figure 1: The location of the 109 meteorological stations (black circular points) and Zhimenda station (black triangle).

Zonal component:

$$Q_\lambda = -\frac{1}{g}\int_{p_s}^{p_t} qu\mathrm{d}p. \tag{2}$$

Meridional component:

$$Q_\phi = -\frac{1}{g}\int_{p_s}^{p_t} qv\mathrm{d}p. \tag{3}$$

In the above equations, g is the gravity acceleration, with a value of 9.80665 m·s^{-2} in this study; Ps is the surface pressure; Pt is the top level pressure (300 hPa in this study); q is the specific humidity; and u and v are the zonal and meridional wind, respectively.

The Pearson correlation coefficient [45] is one of the most commonly used statistical tools to measure the degree of linear correlation between two given variables. The correlation coefficient between two variables—$x_1, x_2, \ldots, x_n$ and $y_1, y_2, \ldots, y_n$—can be calculated as follows:

$$R = \frac{\sum_{i=1}^{n}(x_i - \overline{x})(y_i - \overline{y})}{\sqrt{\sum_{i=1}^{n}(x_i - \overline{x})^2}\sqrt{\sum_{i=1}^{n}(y_i - \overline{y})^2}}. \tag{4}$$

The overbars represent the climatological mean. In this correlation calculation, the runoff in the flood season is the sum of monthly runoff from July to September, the rainfall is the sum of daily rainfall from 16 June to 15 September, and the circulation is the average of the daily data from 16 June to 15 September. The correlation coefficient value is located in the range from −1 to 1. A positive correlation with a value greater than 0 means that the two variables change in a similar direction (i.e., both variables increase or decrease). In addition, a negative correlation with a value less than 0 implies that the two variables exhibit opposite changes (i.e., as one variable increases, the other decreases).

The station data were interpolated to the grid data by the Cressman interpolation technique [46]. Multiple passes are made through the grid with increasingly smaller radii of influence. At each pass, a new value is calculated for each grid point based on a correction factor that is determined by looking at each station within the radius of influence. For each such station, an error is defined as the difference between the station value and a value arrived by interpolation from the grid to that station. A distance-weighted formula is then applied to all such errors within the radius of influence of the grid point to arrive at a correction value for that grid point. The correction factors are applied to all grid points before the next pass is made. Observations nearest to the grid point carry the most weight. As the distance increases, the observations carry less weight. The Cressman function in Ingrid calculates the weights as follows:

$$W = \frac{R^2 - r^2}{R^2 + r^2}, \tag{5}$$

where W is the influence radius and r is the distance between the station and the grid point.

3. Characteristics of Changes in Runoff in the SRYR

3.1. Annual Distribution of Runoff in the SRYR. Figure 2 shows the monthly variation in the runoff at the Zhimenda station. As shown in Figure 2, relatively high runoff occurs between June and October. In particular, the highest runoff occurs between July and September. The total runoff in these three months accounts for 59.6% of the total annual runoff. In contrast, the runoff at the Zhimenda station is notably lower between January and March and in December. Changes in runoff at the Zhimenda station during the flood season (i.e., from July and September) directly affect the annual changes, and the changes also have a significant impact on the regional ecological environment. Hence, this study focuses mainly on analyzing the runoff in the SRYR between July and September.

3.2. Changes in Runoff in the SRYR during the Flood Season. Figure 3 shows the time series of the runoff at Zhimenda station in the flood season during 1971–2012. Overall, the runoff at the Zhimenda station during the flood season displays a slight increasing, albeit insignificant, trend. The runoff at the Zhimenda station during the flood season increased in the early 1970s, decreased in the late 1970s, and was generally high between the 1980s and the mid-1990s. The runoff significantly increased between the mid-1990s (approximately 1994) and 2012 and has been high since 2005, reaching its highest level in 2009. Evidently, there are notable trends of interannual and interdecadal changes in runoff in the SRYR.

4. Correlation Analysis of Runoff and Rainfall in the SRYR during the Flood Season

Some research shows that climate change in the eastern TP has a significant impact on water resources in the upper

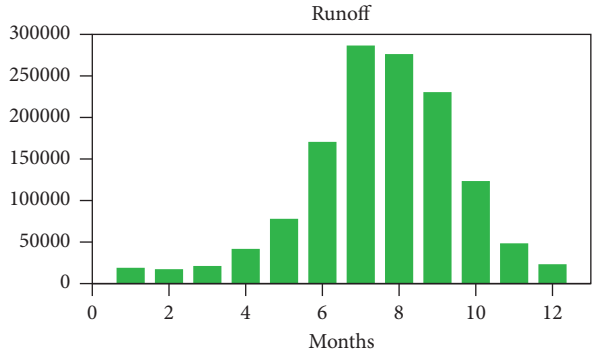

Figure 2: Monthly variation in the runoff at the Zhimenda station (units: $\times 10^4$ m^3).

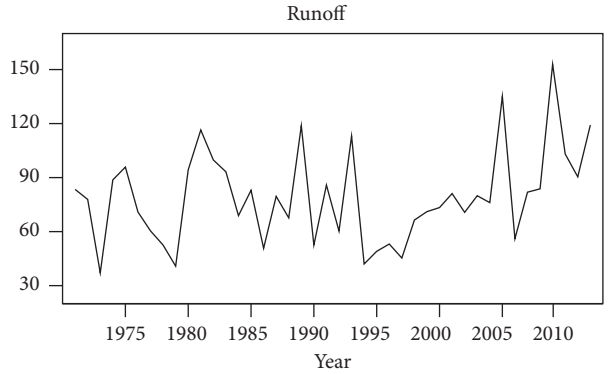

Figure 3: The time series of the runoff at Zhimenda station in the flood season during 1971–2012 (unit: $\times 10^8$ m^3).

reaches of the Yangtze River and that the annual runoff in the upper reaches of the Yangtze River increases as the precipitation in the eastern TP increases [47]. Thus, the rainfall has a significant impact on runoff. Therefore, this section focuses mainly on examining the impact of rainfall on runoff in the SRYR during the flood season.

The runoff is not only affected by simultaneous rainfall but is also affected by antecedent rainfall [48]. Thus, a lag correlation between rainfall and runoff with the daily rainfall leading runoff by 15 days (for June 16 to September 15) is calculated (Figure 4). From Figure 4, it is seen that there is a significant positive correlation over central and southern Qinghai Province, including from the city of Golmud eastward to the large region to the west of the Golog and Hainan Tibetan Autonomous Prefectures, as well as northwestern Sichuan Province. The correlation regions with correlation coefficients greater than 0.6 are mainly distributed in the coastal zone of the SRYR upstream of the Zhimenda station and the two centers over the Tuotuo River region and Qumarleb. Note that lag correlations between rainfall and runoff with other leading times (e.g., 30, 25, 20, 10, and 5 days) were also calculated (not shown). The results show that the significant positive correlation region is highly similar to Figure 4, but the regional ranges of correlation coefficients greater than 0.7 are obviously smaller than that in Figure 4. The above evidence suggests that the rainfall leading runoff by 15 days is reasonable. Therefore, more

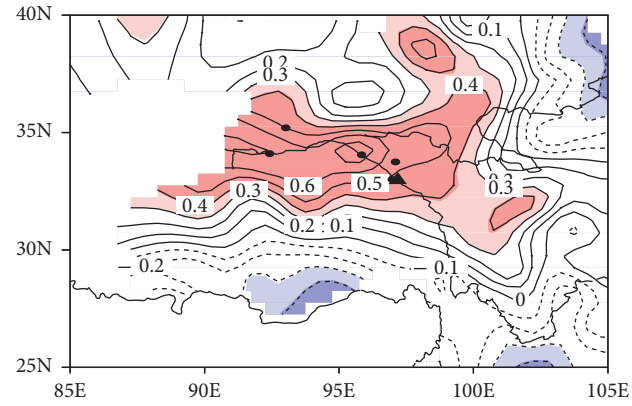

Figure 4: The lag correlation between rainfall and runoff at the Zhimenda station with rainfall leading runoff by 15 days. The dark (light) shading indicates the correlation coefficients significant at the 99% (95%) confidence level. The black circular points represent five meteorological stations that were selected in Section 5. The black triangle represents the Zhimenda station.

attention should be paid to the 15-day antecedent rainfall when examining the impact of rainfall on runoff in the SRYR during the flood season. In the following sections of the analysis of the impact of atmospheric circulation patterns on rainfall in the SRYR, the data for the period between June 16 and September 15 (a 15-day antecedent period of runoff) are examined.

5. Impact of the WJ on Rainfall in the SRYR

The aforementioned analysis shows a significant correlation between changes in runoff in the SRYR and the 15-day antecedent rainfall in the coastal zone of the SRYR. The SRYR is situated in the WJ-affected region. Does the WJ have an impact on rainfall in the coastal zone of the SRYR? This section focuses mainly on analyzing the impact of the WJ on rainfall in the SRYR.

To analyze the relationship between the WJ and rainfall in the coastal zone of the SRYR, five stations (i.e., Wudaoliang, Tuotuohe, Qumalai, Yushu, and Qingshuihe) were selected (the black circular points in Figure 4). We define a rainfall index (I_r for short) as the mean flood season rainfall of the five stations, and the formula is shown as follows:

$$I_r = \frac{1}{n}\sum_{i=1}^{n} x_i, \tag{6}$$

where n is the number of stations and x is the flood season rainfall, which is defined as the sum of the rainfall from 16 June to 15 September. Figure 5 displays the correlation pattern of the 200 hPa zonal winds with I_r. There is a significant positive correlation between approximately 30°N and 40°N from the Iranian Plateau to the west of the Hetao Plain in China, and the center has a correlation coefficient greater than 0.6 over the western TP eastward toward the central and northern TP. To the north of this significant positive region, from the East European Plain to the West Siberian Plain, there is a significant negative correlation,

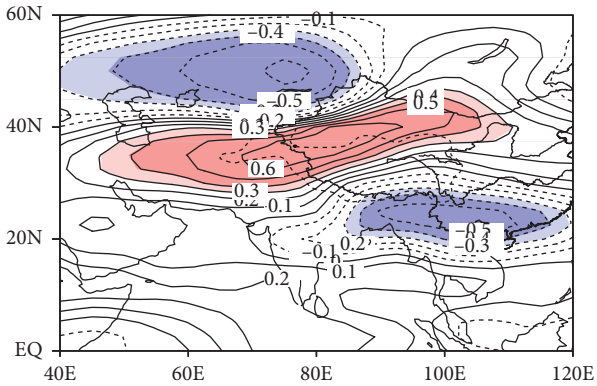

Figure 5: Simultaneous correlation between I_r and the zonal winds at 200 hPa. The dark (light) shading indicates the correlation coefficient significant at the 99% (95%) confidence level.

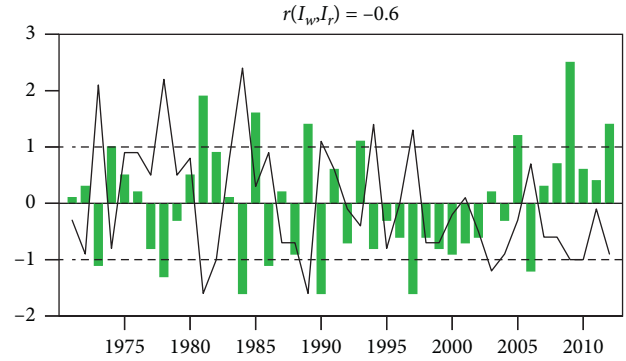

Figure 6: Normalized time series of the I_W (solid curve) and I_r (green bars).

with the center (correlation coefficient less than −0.6) over the central West Siberian Plain. Another significant negative correlation region is situated from the north of the Bay of Bengal eastward to South China. This suggests that when there are positive (negative) anomalies of the 200 hPa zonal winds over Iranian Plateau extending eastward toward the Hetao Plain in China and negative (positive) anomalies of the 200 hPa zonal winds over the East European and West Siberian plains, which result in increased (decreased) rainfall in the coastal zone of the SRYR. Therefore, the upper-level WJ has a close relationship with rainfall in the coastal zone of the SRYR.

The northward and southward jumps of the upper-level WJ have a significant impact on rainfall [23, 34, 35]. Lin [49] noted that the jumps of an upper-level jet are related to the intensity of the westerly winds north of the jet. Therefore, a WJ intensity index (I_W) is defined as the area-mean 200 hPa zonal winds over 45–55°N and 55–85°E. In addition, the jet position index (I_L) is defined as the latitude averaged within 55–85°E, and the latitude is the location of the maximum 200 hPa zonal winds every 2.5° of longitude. A small (large) I_L indicates that the jet is at a relatively low (high) position. The correlation coefficient between I_W and I_L reached 0.904, which was significant at the 99% confidence level. Note that the results obtained are very similar for the reasonable change in the regions used to define I_W and I_L. Clearly, the magnitude of I_W can satisfactorily reflect the southward and northward movements of the WJ. In other words, when the WJ over the key region is relatively strong (weak), the WJ is located relatively northward (southward). Thus, the impact of I_W on rainfall is mainly analyzed in the following.

Will changes in the intensity of the WJ over the selected key region affect rainfall anomalies in the coastal zone of the SRYR? Figure 6 displays the normalized time series of I_W and I_r. The temporal correlation coefficient between them is as high as −0.6 and is significant at the 99% confidence level. Clearly, when I_W is relatively low, I_r is relatively high, indicating relatively heavy rainfall, particularly in 1981, 1989 and 2009. In contrast, when I_W is relatively high, I_r is relatively low, indicating abnormally light rainfall, particularly in 1973, 1978, 1984, 1990, and 1997.

The simultaneous correlation coefficients between I_W and rainfall were further calculated (Figure 7(a)). From Figure 7(a), the significant negative correlation is distributed along the coast of the upper reaches of the Yangtze River, with a center (with a correlation coefficient less than −0.5) over the region near the Tuotuo River. In addition, high-I_W (low-I_W) years are defined as years when the normalized I_W is greater (less) than 1 (−1). Based on these criteria, six years, including 1973, 1978, 1984, 1990, 1994, and 1997, are identified as high-I_W years, and another six years, i.e., 1981, 1982, 1989, 2003, 2009, and 2010, are identified as low-I_W years. Figure 7(b) shows the composite anomalies of rainfall between the high-I_W and low-I_W years. Pronounced negative rainfall anomalies are observed over the coastal zone in the upper reaches of the Yangtze River, with an amplitude of approximately 90 mm. The results are similar to those in Figure 7(a). The above evidence suggests that when above-normal (below-normal) zonal winds occur over the key region, the rainfall in the coastal zone of the SRYR decreases (increases). Thus, changes in the intensity of the WJ over the key region indeed have an impact on rainfall in the coastal zone of the SRYR.

6. Impact of the Intensity of the WJ over the Key Region on Atmospheric Circulation Patterns

The analysis in the previous section shows that changes in the intensity of the WJ over the key region have a significant impact on rainfall anomalies in the coastal zone of the SRYR. What is the mechanism of impact? This section focuses mainly on analyzing the impact of changes in the intensity of the WJ over the key region on the zonal and meridional vertical circulation patterns.

6.1. Impact of the Intensity of the WJ over the Key Region on the Zonal Vertical Circulation. Figure 8(a) shows the simultaneous correlation between I_W and the zonal vertical circulation averaged over 30–37.5°N. As shown in Figure 8(a), the SRYR is dominated by descending air motion. Additionally, there are significant easterly winds from the surface to 100 hPa over the region to the west of the SRYR. However, no significant correlation is observed over the region to the

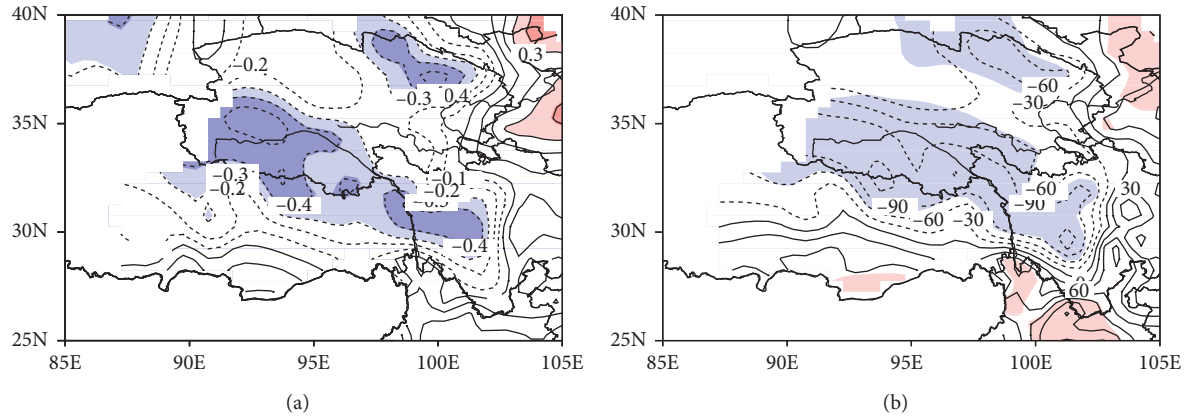

Figure 7: (a) Simultaneous correlation between I_W and rainfall. (b) Composite anomalies of the rainfall between the high-I_W and low-I_W years. The dark (light) shading in (a) indicates correlation coefficients significant at the 99% (95%) confidence level. The shading in (b) indicates rainfall anomalies significant at the 95% confidence level.

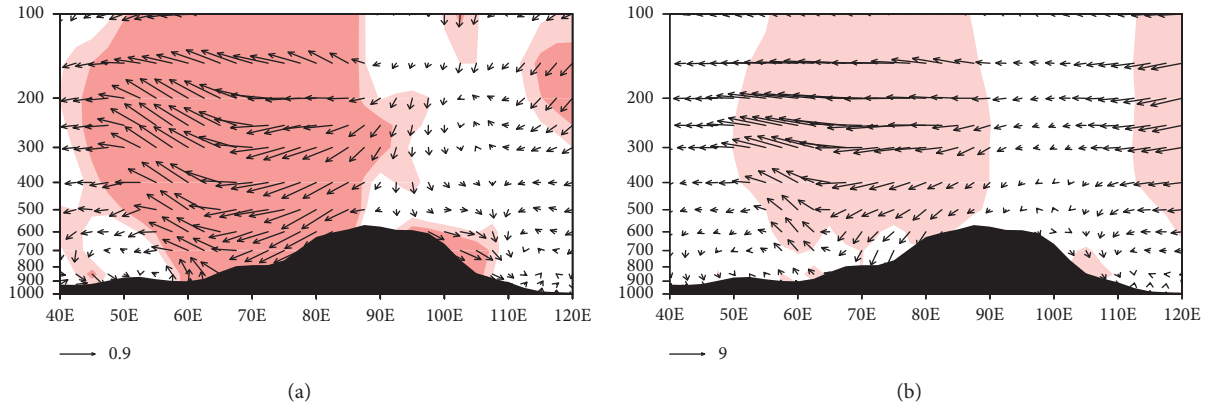

Figure 8: (a) Simultaneous correlation between I_W and the zonal vertical circulation averaged over 30–37.5°N. (b) Composite anomalies of the zonal vertical circulation averaged over 30–37.5°N between the high-I_W and low-I_W years. The dark (light) shading in (a) indicates the correlation coefficients significant at the 99% (95%) confidence level. The shading in (b) indicates the zonal vertical circulation anomalies significant at the 95% confidence level.

east of the SRYR. In addition, Figure 8(b) shows composite anomalies of the zonal vertical circulation averaged over 30–37.5°N between the high-I_W and low-I_W years. From Figure 8(b), pronounced descending motion anomalies over the SRYR and significant easterly wind anomalies over the region to the west of the SRYR are observed. The results are similar to those in Figure 8(a). The above evidence implies that when the I_W is greater (less) than the normal value, the WJ position moves northward (southward), which results in significant easterly (westerly) wind anomalies over the region to the west of the SRYR and significant descending (ascending) motion anomalies over the SRYR.

6.2. Impact of the Intensity of the WJ over the Key Region on the Meridional Vertical Circulation. Figure 9(a) shows the simultaneous correlation between I_W and the meridional vertical circulation averaged over 90–100°E. As shown in Figure 9(a), there is significant meridional circulation over the region between 25°N and 35°N, and its descending branch is situated over the SRYR, which would result in a significant descending motion of northerly winds over the SRYR. There is another enormous meridional circulation over the equatorial region, and its ascending branch coincides with the ascending branch of the meridional circulation over the region between 25°N and 35°N, resulting in significant ascending motion in the air flow over the region between 5°N and 27°N. Consequently, the majority of the southerly winds in the lower meridional circulation over the equatorial region transform to ascending air currents when advancing northward and thus can no longer continue to move northward; only a small portion of these southerly winds continue to move northward. However, because of the presence of a small meridional circulation in the lower atmosphere between 20°N and 25°N, these northward-moving southerly winds transform into descending air currents and thus can no longer move northward when reaching approximately 25°N. This circulation pattern is unfavorable to continued northward movement of the southerly wind toward the SRYR. In addition, Figure 9(b) shows composite anomalies of the meridional vertical circulation averaged over 90–100°E between the high-I_W and low-I_W years, and

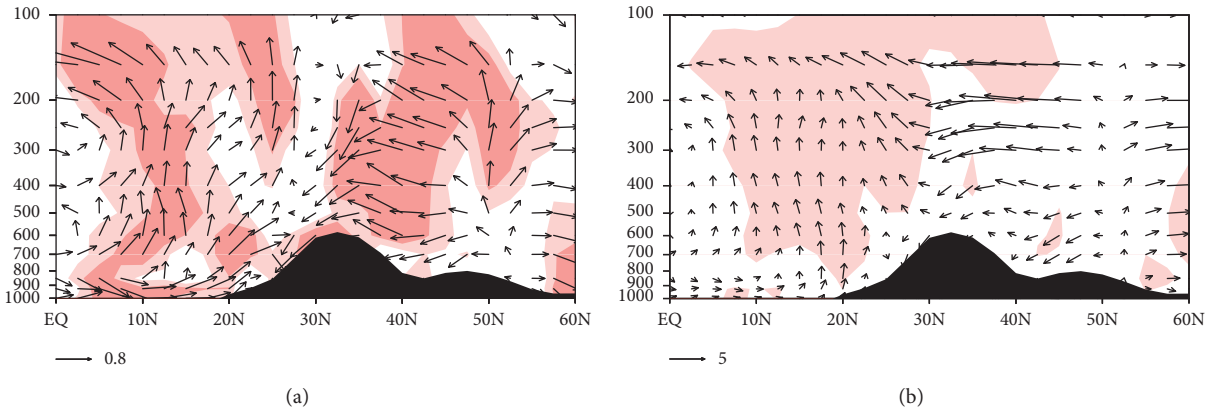

FIGURE 9: (a) Simultaneous correlation between I_W and the meridional vertical circulation averaged over 90–100°E. (b) Composite anomalies of the meridional vertical circulation averaged over 90–100°E between the high-I_W and low-I_W years. The dark (light) shading in (a) indicates the correlation coefficients significant at the 99% (95%) confidence level. The shading in (b) indicates the meridional vertical circulation anomalies significant at the 95% confidence level.

the results are similar to those in Figure 9(a). Thus, when the I_W is greater (less) than the normal value, the southerly wind over the equatorial region cannot (can) easily advance northward, and significant descending (ascending) motion anomalies occur over the SRYR.

6.3. Possible Impact Mechanism. Figure 10(a) shows the correlation between the I_W and the 200 hPa winds and divergence field. From Figure 10(a), there is significant cyclonic circulation over the TP, with significant convergence over the TP. Meanwhile, in the lower level (i.e., 600 hPa, Figure 10(b)), significant anticyclonic circulation and significant divergence occur over the TP. Note that the results of the composite anomalies of the winds and divergence fields at 200 hPa and 600 hPa between the high-I_W and low-I_W years (Figures 10(c) and 10(d)) are similar to Figures 10(a) and 10(b). The above evidence implies that the jet position moves northward (southward) when there are positive (negative) anomalies of the I_W, negative (positive) 200 hPa zonal wind anomalies over the region from 30°N to 40°N, and positive (negative) anomalies over the area south of the sources of three rivers (i.e., Lancang River, Yellow River and Yangtze River), which result in upper-level cyclonic (anticyclonic) shear anomalies over the TP. In addition, for the 600 hPa zonal winds, positive (negative) anomalies over the area north of the sources of three rivers and negative (positive) anomalies over area south of the sources of the three rivers result in low-level anticyclonic (cyclonic) shear anomalies over the TP. Hence, the convergence (divergence) anomalies in the upper level and the divergence (convergence) anomalies in the lower level are induced by the cyclonic (anticyclonic) circulation and anticyclonic (cyclonic) circulation anomalies, respectively. These processes result in descending (ascending) motion anomalies over the SRYR, which decrease (increase) rainfall. Hence, these circulation patterns also impact runoff. Because runoff has a close relationship with rainfall, circulation anomalies indirectly impact runoff by impacting rainfall. When the antecedent rainfall decreases (increases) in the SRYR during the flood season, runoff also decreases (increases).

7. Impact of the Intensity of the WJ over the Key Region on Water Vapor Transport

Water vapor is the source of rainfall. Water vapor is transported to a rainfall region by large-scale air movement and, when facilitated by a specific circulation pattern, ascends and cools to form clouds, which in turn generate rainfall. The SRYR is situated in the eastern TP. Water vapor transport is particularly vital to rainfall in the SRYR. The analysis in the previous section shows that changes in the intensity of the WJ over the key region affect rainfall in the coastal zone of the SRYR by affecting the atmospheric circulations. How do the changes in this circulation pattern affect water vapor? This section focuses mainly on analyzing the impact of the intensity of the WJ over the key region on water vapor transport.

Figure 11(a) shows the simultaneous correlation between I_W and vertically integrated water vapor flux. From Figure 11(a), there is a significant anticyclonic water vapor transport over the region extending from the Caspian Sea eastward to the western TP, and the southerly water vapor transport on its western side is unfavorable to the southward transport of the water vapor from the Caspian Sea region. The majority of the westerly water vapor is transported eastward and transforms into southwesterly water vapor on the northern side of the anticyclonic water vapor transport, which is unfavorable to the southward transport of water vapor originating from high latitudes. The rest of the westerly water vapor transforms into northwesterly water vapor, which continues to be transported eastward. During the eastward transport process, some of the northwesterly water vapor is transported to Northeast China along the northern edge of the TP via the Hetao region. The remainder transforms into northeasterly water vapor and converges over the southern edge of the TP with the easterly water vapor transported from Taiwan Province to the south of the

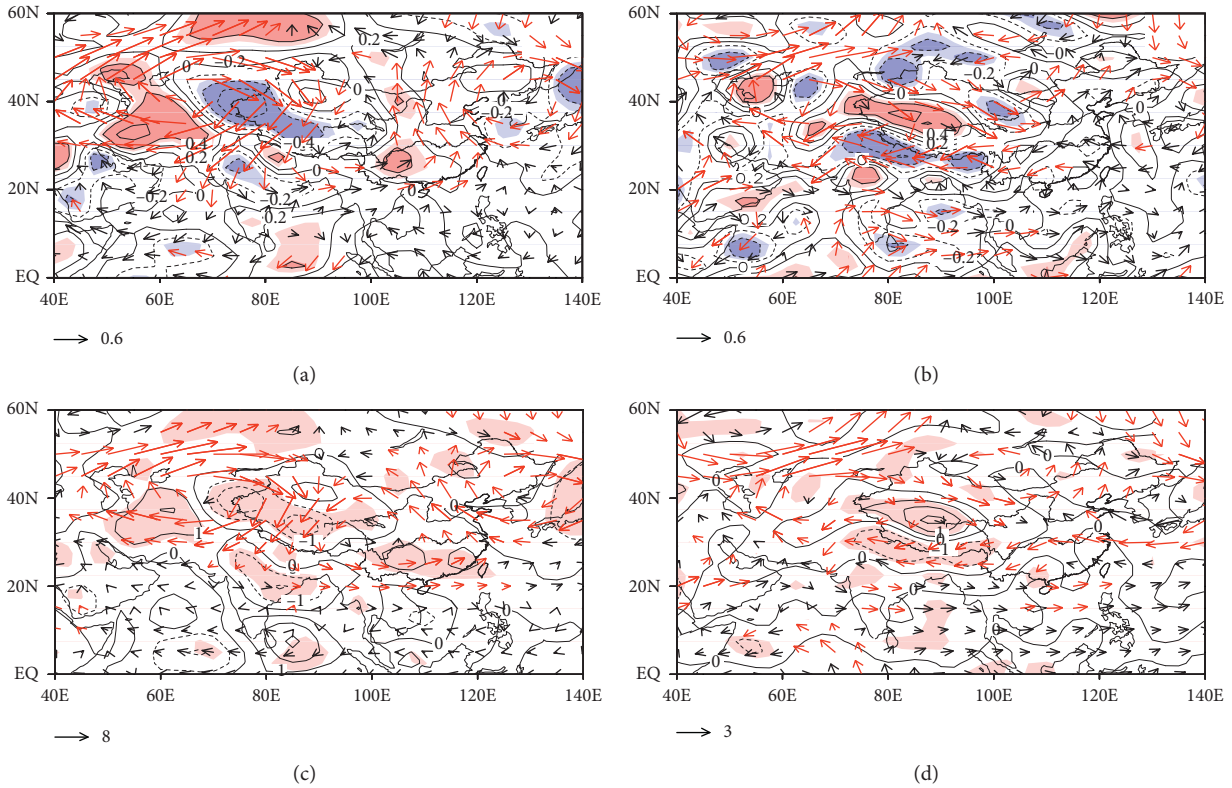

Figure 10: Correlation between the I_W and the winds and divergence field (contours) at (a) 200 hPa and (b) 600 hPa. Composite anomalies of the winds and divergence field (contour) at (c) 200 hPa and (d) 600 hPa between the high-I_W and low-I_W conditions. The dark (light) shading in (a) and (b) indicates the correlation coefficients significant at the 99% (95%) confidence level. The shading in (c) and (d) indicates the divergence anomalies significant at the 95% confidence level. The red wind vectors indicate the zonal or meridional wind at the 95% confidence level.

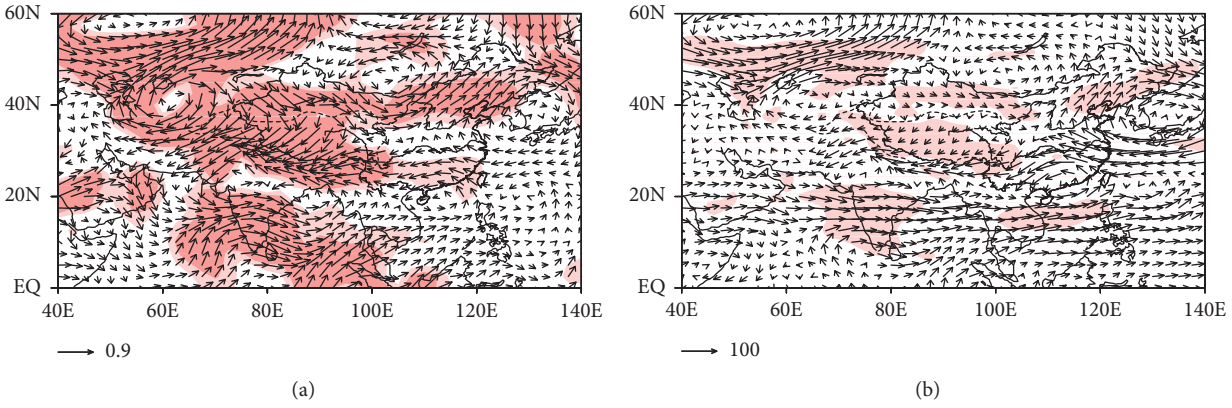

Figure 11: (a) Simultaneous correlation between I_W and vertically integrated water vapor flux. (b) Composite anomalies of the water vapor fluxes between the high-I_W and low-I_W years (unit: g·(s·cm)$^{-1}$). The dark (light) shading in (a) indicates the correlation coefficients significant at the 99% (95%) confidence level. The shading in (b) indicates the water vapor flux anomalies significant at the 95% confidence level.

TP via South China and then is transported westward, which obviously is unfavorable for the westerly water vapor to be transported to the SRYR. There is also another significant westerly water vapor transport over the region extending from the low-latitude Indian Ocean to the region west of the Indochina peninsula, which is also unfavorable to the transport of water vapor from the low-latitude ocean to the SRYR. As a result, there is a decrease in the water vapor content over the SRYR. Figure 11(b) shows composite anomalies of the water vapor fluxes between the high-I_W and low-I_W years. As shown in Figure 11(b), the significant anticyclonic water transport anomalies over the region

extending from the Caspian Sea eastward to the western TP are unfavorable to the southward transport of water vapor originating from high-latitude regions. The significant westerly water vapor transport anomalies from the Arabian Sea via the Indian subcontinent are unfavorable to the northward transport of water vapor originating from the low-latitude ocean. The results are similar to those in Figure 11(a). Thus, changes in the intensity of the WJ over the key region have a significant impact on water vapor transport. When there are positive (negative) I_W anomalies, the water vapor content of the SRYR decreases (increases).

The above evidence indicates that when the I_W is greater (less) than the normal value, the WJ shifts northward (southward). In response, the easterly (westerly) wind anomalies over the region to the west of the SRYR become unfavorable (favorable) to the transport of water vapor from high-latitude regions to the SRYR, and the westerly (easterly) water vapor transport anomalies over the Arabian Sea also become unfavorable (favorable) to the northward transport of water vapor originating from the low-latitude ocean. Thus, the water vapor content over the SRYR decreases (increases). In addition, the anomalies descending (ascending) motion occur over the SRYR. These factors decrease (increase) the rainfall in the coastal zone of the SRYR. Additionally, these factors indirectly impact runoff by impacting rainfall; for example, a decrease (increase) in antecedent rainfall decreases (increases) the runoff in the SRYR during the flood season.

8. Conclusions and Discussion

Using runoff data from the Zhimenda station, this study analyzes the characteristics of changes in runoff in the SRYR during the flood season (from July to September) and its relationship with antecedent rainfall in the SRYR and further analyzes the impact of the WJ on rainfall in the coastal zone of the SRYR. The main conclusions derived from this study are summarized as follows.

(1) Changes in runoff in the SRYR during the flood season display notable interdecadal characteristics. The runoff in the SRYR during the flood season increased in the early 1970s, decreased in the late 1970s, slowly decreased between the 1980s and the mid-1990s, and significantly increased between the mid-1990s (approximately 1994) and 2012.

(2) Fifteen-day antecedent rainfall in the coastal zone of the SRYR (i.e., June 16 to September 15) is the principal factor that affects the runoff in the SRYR during the flood season.

(3) There is a close relationship between rainfall in the coastal zone of the SRYR and the intensity of the WJ over the key region (55–85°E, 45–55°N). When the WJ over the key region is relatively strong (weak), rainfall in the coastal zone of the SRYR decreases (increases).

(4) When there are positive (negative) anomalies of the I_W, the jet position moves northward (southward) and the easterly (westerly) wind anomalies over the region to the west of the SRYR become unfavorable (favorable) to the transport of water vapor from high-latitude regions to the SRYR. In addition, the southerly wind over the equatorial region cannot (can) easily advance northward, which results in a westerly (easterly) water vapor transport anomalies over the Arabian Sea, which is unfavorable (favorable) to the northward transport of water vapor from the low-latitude ocean. Hence, these conditions decrease (increase) the water vapor content over the SRYR.

(5) When the I_W is greater (less) than the normal value, convergence (divergence) anomalies in the upper level (i.e., 200 hPa) and divergence (convergence) anomalies in the lower level (i.e., 600 hPa) are induced by the cyclonic (anticyclonic) and anticyclonic (cyclonic) circulation anomalies, respectively. These circulation patterns result in descending (ascending) motion anomalies over the SRYR. In addition, the water vapor content over the SRYR decreases (increases). These conditions decrease (increase) rainfall, resulting in less (more) runoff in the SRYR during the flood season.

This study analyzes the impact of the WJ on rainfall in the SRYR from only a statistical perspective. The results require further validation through numerical simulation. In addition, there are a myriad of factors that affect the rainfall in the SRYR, and this study only focuses on analyzing the impact of the WJ. Other factors, such as the plateau monsoon and South Asian High, also, to a certain extent, affect rainfall in the SRYR. Therefore, changes in the intensity of the WJ do not coincide with changes in rainfall in the SRYR in some years with abnormally heavy or light rainfall. Hence, the interactions between various factors will be fully taken into consideration in future work.

Data Availability

The data used to support the findings of this study are available from the corresponding author upon request.

Conflicts of Interest

The authors declare no conflicts of interest.

Acknowledgments

This research was funded by the Opening Fund of Key Laboratory for Land Surface Process and Climate Change in Cold and Arid Regions, Chinese Academy of Sciences (grant no. LPCC2016004), Open Research Fund Program of Plateau Atmosphere and Environment Key Laboratory of Sichuan Province (grant number PAEKL-2018-K2), the Scientific Research Foundation of Chengdu University of Information Technology (grant no. J201711), and the National Natural Science Foundation of China (grant nos. 91537214, 41775079, and 41905008).

References

[1] J. Yang, Y. Ding, and R. Chen, "Climatic causes of ecological and environmental variations in the source regions of the Yangtze and Yellow rivers of China," *Environmental Geology*, vol. 53, no. 1, pp. 113–121, 2007.

[2] Y. Zhang, S. Liu, J. Xu, and D. Shangguan, "Glacier change and glacier runoff variation in the Tuotuo River basin, the source region of Yangtze River in Western China," *Environmental Geology*, vol. 56, no. 1, pp. 59–68, 2008.

[3] L. Bing, Q. Shao, and J. Liu, "Runoff characteristics in flood and dry seasons based on wavelet analysis in the source regions of the Yangtze and Yellow rivers," *Journal of Geographical Sciences*, vol. 22, no. 2, pp. 261–272, 2012.

[4] Y. Zhang, S. Zhang, J. Xia, and D. Hua, "Temporal and spatial variation of the main water balance components in the three rivers source region, China from 1960 to 2000," *Environmental Earth Sciences*, vol. 68, no. 4, pp. 973–983, 2013.

[5] Y. Zhang, S. Zhang, X. Zhai, and J. Xia, "Runoff variation and its response to climate change in the three rivers source region," *Journal of Geographical Sciences*, vol. 22, no. 5, pp. 781–794, 2012.

[6] H. Y. Yan, G. L. Yang, and Q. C. Wang, "Change of annual runoff distribution in the headwaters of the Yangtze river," *Journal of Glaciology and Geocryology*, vol. 28, no. 4, pp. 526–529, 2006.

[7] L. Y. Jin, N. S. Qin, and X. L. Mao, "Features of runoff in the up reaches of the Tongtian river and its climatic probobility forecast in recent 45 years," *Climatic and Environmental Research*, vol. 10, no. 2, pp. 220–228, 2005.

[8] X. H. Shi, N. S. Qin, W. J. Xv et al., "The variations characteristic of the runoff in the source regions of the Yangtze river from 1956 to 2004," *Journal of Mountain Science*, vol. 25, no. 5, pp. 513–523, 2007.

[9] Y. S. Sun, Y. Q. Duan, Y. Li, and G. C. Cao, "Variation characteristics and trend analysis of runoff at the source regions of the three river in Qinghai during recent years," *Journal of Water Resources & Water Engineering*, vol. 26, no. 1, pp. 52–57, 2015.

[10] N. S. Qin, L. Y. Jin, X. H. Shi et al., "A 518-year runoff reconstruction of Tongtian river basin using tree-ring width chronologies," *ActaGeographicaSinica*, vol. 59, no. 4, pp. 550–556, 2004.

[11] S. Zhang, D. Hua, X. Meng, and Y. Zhang, "Climate change and its driving effect on the runoff in the "Three-River Headwaters" region," *Journal of Geographical Sciences*, vol. 21, no. 6, pp. 963–978, 2011.

[12] S. Wu, Z. Yao, H. Huang, Z. Liu, and Y. Chen, "Glacier retreat and its effect on stream flow in the source region of the Yangtze River," *Journal of Geographical Sciences*, vol. 23, no. 5, pp. 849–859, 2013.

[13] L. Li, H. Shen, S. Dai, H. Li, and J. Xiao, "Response of water resources to climate change and its future trend in the source region of the Yangtze River," *Journal of Geographical Sciences*, vol. 23, no. 2, pp. 208–218, 2013.

[14] L. J. Wang and H. Y. Yan, "Analysis of impacting factor on change of annual runoff distribution in head-water area of the Yangtze River," *Journal of Water Resources & Water Engineering*, vol. 22, no. 1, pp. 174–176, 2011.

[15] L. Li, Z. Y. Wang, N. S. Qin, and Y. C. Ma, "Analysis of the relationship between runoff amount and its impacting factor in the upper Yangtze river," *Journal of Natural Resources*, vol. 19, no. 6, pp. 694–700, 2004.

[16] Q. C. Liu, N. S. Qin, J. W. Xv, X. H. Shi, Q. C. Wang, and S. Q. Feng, "Response of runoff to interannual climate change over Changjiang river source region," *Meteorological Science and Technology*, vol. 36, no. 3, pp. 277–280, 2008.

[17] C. W. Xie and S. H. Qi, "Analysis of runoff change and its response to weather fluctuation at source regions of the Yangtze and Yellow rivers," *Resources and Environment in the Yangtze Basin*, vol. 16, no. 2, pp. 251–255, 2007.

[18] S. Xuan, Q. Zhang, and S. Sun, "Anomalous midsummer rainfall in Yangtze River-Huaihe River valleys and its association with the East Asia westerly jet," *Advances in Atmospheric Sciences*, vol. 28, no. 2, pp. 387–397, 2011.

[19] S. Wang and H. Zuo, "Effect of the east asian westerly jet's intensity on summer rainfall in the Yangtze River valley and its mechanism," *Journal of Climate*, vol. 29, no. 7, pp. 2395–2406, 2016.

[20] S. Wang, H. Zuo, S. Zhao, J. Zhang, and S. Lu, "How East Asian westerly jet's meridional position affects the summer rainfall in Yangtze-Huaihe River Valley?" *Climate Dynamics*, vol. 51, no. 11-12, pp. 4109–4121, 2018.

[21] T. Sampe and S.-P. Xie, "Large-scale dynamics of the Meiyu-Baiu rainband: environmental forcing by the westerly jet," *Journal of Climate*, vol. 23, no. 1, pp. 113–134, 2010.

[22] Y. Zhao, X. J. Yu, J. Q. Yao, and X. N. Dong, "Evaluation of the subtropical westerly jet and its effects on the projected summer rainfall over central Asia using multi-CMIP5 models," *International Journal of Climatology*, vol. 38, pp. 1176–1189, 2018.

[23] Y. Zhang and L. L. Guo, "Relationship between the simulated East Asian westerly jet biases and seasonal evolution of rainbelt over eastern China," *Chinese Science Bulletin*, vol. 50, no. 14, pp. 1503–1508, 2005.

[24] D. Z. Ye, S. Y. Tao, and M. C. Li, "The abrupt change of atmospheric circulation over the northern hemisphere during June and October," *ActaMeteorologicaSinica*, vol. 29, pp. 249–263, 1958.

[25] X. Y. Kuang and Y. C. Zhang, "Seasonal variation of the East Asia subtropical westerly jet and its association with the heating field over East Asia," *Advances in Atmospheric Sciences*, vol. 22, no. 6, pp. 831–840, 2005.

[26] Z. D. Lin and R. Y. Lu, "Interannualmeridional displacement of the East Asia upper-tropospheric jet stream in summer," *Advances in Atmospheric Sciences*, vol. 22, pp. 199–211, 2005.

[27] Z. Lin, Y. Fu, and R. Lu, "Intermodel diversity in the zonal location of the climatological East Asian westerly jet core in summer and association with rainfall over East Asia in CMIP5 models," *Advances in Atmospheric Sciences*, vol. 36, no. 6, pp. 614–622, 2019.

[28] M. Kwon, J.-G. Jhun, and K.-J. Ha, "Decadal change in east Asian summer monsoon circulation in the mid-1990s," *Geophysical Research Letters*, vol. 34, no. 21, p. L21706, 2007.

[29] S. Yang, K.-M. Lau, and K.-M. Kim, "Variations of the east asian jet stream and asian-Pacific-American winter climate anomalies," *Journal of Climate*, vol. 15, no. 3, pp. 306–325, 2002.

[30] N. Wang and Y. Zhang, "Connections between the Eurasian teleconnection and concurrent variation of upper-level jets over East Asia," *Advances in Atmospheric Sciences*, vol. 32, no. 3, pp. 336–348, 2015.

[31] S. Y. Tao, Y. J. Zhao, and X. M. Chen, "The relationship between May-Yü in far east and the behavior of circulation over Asia," *ActaMeteorologicaSinica*, vol. 29, no. 2, pp. 119–134, 1958.

[32] C. Y. Li, Z. T. Wang, S. Z. Lin, and H. R. Cho, "The relationship between East Asian summer monsoon activity and northward jump of the upper westerly jet location," *Chinese Journal of Atmospheric Sciences*, vol. 8, no. 5, pp. 641–658, 2004.

[33] R. Lu, "Associations among the components of the east asian summer monsoon system in the meridional direction," *Journal of the Meteorological Society of Japan*, vol. 82, no. 1, pp. 155–165, 2004.
[34] L. N. Dong, P. W. Guo, P. X. Wang, and L. Qi, "Impacts of the variation of westerly jets over East Asia in july on the precipitation of East China," *Plateau Meteorology*, vol. 29, no. 2, pp. 286–296, 2010.
[35] H. Q. Liao, S. T. Gao, H. J. Wang, and S. Y. Tao, "Anomalies of the extratropical westerly jet in the north hemisphere and their impacts on East Asia summer monsoon climate anomalies," *Chinese Journal of Geophysics*, vol. 47, no. 1, pp. 10–18, 2004.
[36] R. Yu, B. Wang, and T. Zhou, "Tropospheric cooling and summer monsoon weakening trend over East Asia," *Geophysical Research Letters*, vol. 31, no. 22, 2004.
[37] B. Z. Shen, Z. D. Lin, R. Y. Lu, and Y. Lian, "Circulation anomalies associated with interannual variation of early- and late-summer precipitation in Northeast China," *Science China Earth Science*, vol. 41, pp. 402–412, 2011.
[38] Y. Zhang, X. Kuang, W. Guo, and T. Zhou, "Seasonal evolution of the upper-tropospheric westerly jet core over East Asia," *Geophysical Research Letters*, vol. 33, no. 11, 2006.
[39] Y. Du, Y. C. Zhang, and Z. Q. Xie, "Impacts of longitude location changes of East Asia westerly jet core on the precipitation distribution during Meiyu period in middle-lower reaches of Yangtze river valley," *ActaMeteorologicaSinica*, vol. 66, no. 4, pp. 566–576, 2008.
[40] L. B. Wei, G. L. Zhou, S. G. Wang, K. Z. Shang, and Y. X. Ma, "Climatic features of Asian upper westerly jet activities and their relationship with summer precipitation in partly areas of China," *Plateau Meteorology*, vol. 31, no. 1, pp. 87–93, 2012.
[41] P. D. Liang and A. X. Liu, "Winter Asia jet stream and seasonal precipitation in east China," *Advances in Atmospheric Sciences*, vol. 11, no. 3, pp. 311–318, 1994.
[42] L. Li and Y. Zhang, "Effects of different configurations of the East Asian subtropical and polar front jets on precipitation during the mei-yu season," *Journal of Climate*, vol. 27, no. 17, pp. 6660–6672, 2014.
[43] Z. F. Fang and L. Zhang, "NCAR-NCEP data quality and abrupt changes of east Asia Low in summer of 1970's," *Plateau Meteorology*, vol. 25, no. 2, pp. 179–189, 2006.
[44] Z. F. Fang, J. Lei, X. N. Lv, X. Qu, and Q. Li, "A comparison of 500 hPa field of East-Asia between the NCEP/NCAR reanalysis data and the ERA-40 of ECMWF data," *ActaMeteorologicaSinica*, vol. 68, no. 2, pp. 270–276, 2010.
[45] K. Pearson, "Mathematical contributions to the theory of evolution III. Regression, heredity, and panmixia," *Philosophical Transactions of the Royal Society of London. Series A*, vol. 187, pp. 253–318, 1896.
[46] G. P. Cressman, "An operational objective analysis system," *Monthly Weather Review*, vol. 87, no. 10, pp. 367–374, 1959.
[47] S. J. Wang, "Climate change over the eastern part of the Tibetan plateau and the impact on water resources in the upper reaches of Yangtze river," *Plateau and Mountain Meteorology Research*, vol. 28, no. 1, pp. 42–46, 2008.
[48] G. Zhuo, J. Jian, and C. R. BianBa, "Runoff of the Jinsha river: characteristics and its response to climate change," *Journal of Glaciology and Geocryology*, vol. 33, no. 2, pp. 405–415, 2011.
[49] Z. D. Lin, "Relationship between meridional displacement of the monthly East Asia jet stream in the summer and sea surface temperature in the tropical central and eastern Pacific," *Atmospheric and Oceanic Science Letters*, vol. 3, pp. 40–44, 2010.